Nanoscale Advances

ROYAL SOCIETY OF CHEMISTRY

MINIREVIEW

View Article Online
View Journal | View Issue

Cite this: *Nanoscale Adv.*, 2020, **2**, 1395

Nanomaterials for the regulation of the tumor microenvironment and theranostics

Wenyao Zhen,[ab] Wenxue Hu,[c] Liang Dong,[d] Shangjie An[ab] and Xiue Jiang *[ab]

Cancer has become one of the primary threats to human beings, and traditional therapies (including surgery, chemotherapy and radiotherapy) show limited therapeutic efficacy due to the complexity of tumor biology. Furthermore, determining how to utilize the differences between the tumor microenvironment (TME) and healthy tissues and exploring new nanoplatforms that can realize early diagnosis and effective and non-toxic therapy are challenges in cancer theranostics. Numerous researchers have designed multifunctional nanomaterials and investigated their personalized therapy and regulation abilities toward TME, including oxygen generation, glutathione consumption and the production of reactive oxygen species and multi-model imaging effects. This review will introduce the latest progress in the design of multi-functional nanomedicines for the regulation of TME and their theranostics, and it will provide a critical angle for the future development of nanomedicine.

Received 31st December 2019
Accepted 8th February 2020

DOI: 10.1039/c9na00816k

rsc.li/nanoscale-advances

1. Introduction

In the last few decades, scientific evidence has identified cancer as one of the leading threats to human beings.[1] However, the non-specificity or excessive radiation of traditional cancer treatments, including chemotherapy, radiation therapy and surgery, can cause collateral damage to healthy cells and tissues. In addition, it is difficult to avoid multidrug resistance and cancer metastasis during the treatment. Thus, it is imperative to overcome the core obstacle of the complex biology of the tumor microenvironment and explore alternative or complementary methods for the accurate localization and effective elimination of tumors. Accordingly, many researchers are trying to find the differences between tumors and healthy tissues because it is generally considered that tumors are abnormal tissues with complex biological microstructures and specific tumor microenvironments (TMEs).[1]

TME is composed of stroma cells, immune cells, extracellular matrices and cancer cells (Fig. 1),[2] which shows quite complex but unique features in angiogenesis, oxygenation and metabolic state.[3] Unlike normal organs, TME usually has an abnormal vasculature, also called hypervascularization and aberrant vascular architecture; also, there is an over-expression of vascular permeability factors, which can stimulate

[a]*State Key Laboratory of Electroanalytical Chemistry, Changchun Institute of Applied Chemistry, Chinese Academy of Sciences, Changchun 130022, Jilin, China. E-mail: jiangxiue@ciac.ac.cn*

[b]*University of Science and Technology of China, Hefei 230026, Anhui, China*

[c]*Department of Materials Science and Engineering, Shenyang University of Chemical Technology, Shenyang 110142, Liaoning, China*

[d]*School of Chemistry and Molecular Engineering, East China Normal University, Shanghai 200241, China*

Wenyao Zhen is now pursing her doctoral degree under the supervision of Prof. Xiue Jiang at the State Key Laboratory of Electroanalytical Chemistry, Changchun Institute of Applied Chemistry (CIAC), Chinese Academy of Sciences. Currently, her research is focused on the design and synthesis of multi-functional nanomaterials with TME-sensitive properties for effective diagnosis and therapeutic systems.

Wenxue Hu is currently pursuing a Master's Degree instructed by Prof. Zhuo Guo at the Department of Materials Science and Engineering, Shenyang University of Chemical Technology. She joined Prof. Jiang's group as a joint graduate student in 2019. Her research interests are the fabrication and applications of functional nanomaterials.

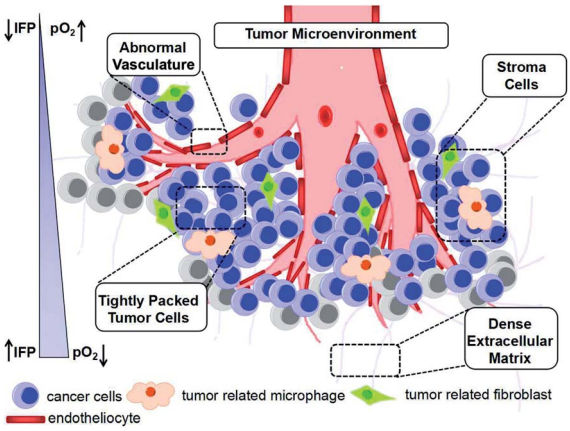

Fig. 1 Schematic illustration of TME. Interstitial fluid pressure (IFP).

extravasation within the tumor tissues. The blood vessels of tumors involve some abnormal openings and defects, which result in the lack of lymphatic drainage. Accordingly, the content of nanomaterials in tumor sites can be several times higher than that in plasma taking advantage of the selective penetration into tumor sites[4] due to their abnormal vascular nature, which is called the enhanced permeability and retention (EPR) effect,[5,6] and it simultaneously provides an entrance for nanomedicines to enter the TME and become entrapped within the tumor tissues. Due to the heterogeneous distribution of tumor vasculatures and the rapid growth of cancer cells, it is difficult for cancer and stromal cells to obtain nutrients and oxygen and thus, most tumor cells have hypoxic regions.[7,8] This hypoxic condition causes tumor cells to adjust themselves to inadequate oxygen and obtain energy through oxygen-independent glycolysis for survival.[4] The rapid metabolism and overproduction of metabolites such as lactic acid and pyruvate accompanied with redundant protons and carbon dioxide lead to a mildly acidic TME (pH: 6.5–6.9),[8–12] enhanced tumor metastasis and treatment resistance.[12–14] Also, the fast metabolism and insufficient blood supply in tumor tissues lead to an elevated content of H_2O_2, accelerated inflammation and tumor metabolism in TME.[15–18] In addition, the concentration of glutathione (GSH), which can regulate the redox balance of TME and protect cells against oxidative damage, in cancer cells is about four-fold that in normal cells,[10,19–21] which has become one of the barriers for reactive oxygen species (ROS)-based therapies, chemotherapy and radiotherapy.[22,23]

The TME not only provides an appropriate environment and nutrition for the development and metastasis of tumors, but also offers a "gate" for selective and effective cancer therapies (Fig. 1). The development of nanotechnology has proven that various nanoplatforms show interesting performances in the early diagnosis and effective treatment of cancer through targeting one or multi-fold characteristics of the TME. Nanomaterials not only can regulate the TME *via* enzyme-like activity, redox reaction and catalysis, but also realize multi-model imaging effects due to their inherent characteristics, including the ferromagnetism, paramagnetism related to

Liang Dong is currently pursuing his Master's Degree under the supervision of Prof. Zhiai Xu and Prof. Wen Zhang at the School of Chemistry and Molecular Engineering, East China Normal University. He joined Prof. Jiang's group as a joint graduate student in 2018. His research interests include the fabrication of functional nanomaterials to load dihydroartemisinin and their applications in cancer diagnosis and treatment.

Shangjie An is currently pursuing her doctoral degree instructed by Prof. Xiue Jiang at the State Key Laboratory of Electroanalytical Chemistry, Changchun Institute of Applied Chemistry (CIAC), Chinese Academy of Sciences. Her research interests include the development of functional nanomaterials and their applications in tumor therapy and diagnosis.

Prof. Xiue Jiang received her Ph.D. degree from Changchun Institute of Applied Chemistry (CIAC), Chinese Academy of Sciences. From 2006 to 2010, she was a Humboldt scholar and Postdoctoral Researcher at the University of Bielefeld, Germany, ULM University in Germany and the Karlsruhe Institute of Technology, Germany. Since 2010 she has been a full Professor at CIAC. Her current research interests include revealing the cellular response mechanisms at the nanoscale by various spectroscopy methods, especially surface-enhanced infrared spectroscopy, for biomedical applications. She has published 85 scientific papers and her h-index is 31.

magnetic resonance imaging (MRI), high X-ray absorption coefficient for computed tomography (CT) imaging, high photothermal conversion efficiency for thermal imaging and photoacoustic imaging (PAI). Herein, this review introduces some strategies (Fig. 2) for cancer theranostics based on different TME responsive nanomaterials (mainly covers the above-mentioned characteristics) and provides essential insight for the future development of nanomedicines.

2. Enhanced chemotheranostics by regulating the TME

Chemotherapy is a therapeutic method that uses highly cytotoxic chemical medicines to suppress the proliferation, infiltration and metastasis of cancer cells until solid tumors are completely destroyed. Cis-platinum, doxorubicin hydrochloride (DOX·HCl), artemisinin and paclitaxel tirapazamine (TPZ) are commonly used chemotherapeutic drugs.[24] Nevertheless, traditional chemotherapy is far from satisfactory, and the adverse results of clinical/preclinical chemotherapy may be ascribed to severe toxic side effects and drug resistance. Thus, in recent years, smart nanomedicines have become attractive platforms for targeted tumor chemotherapy, which can achieve effective accumulation inside tumors after reasonable design, provide the opportunity to increase therapeutic efficiency and reduce the defects of traditional chemotherapy. Drug-loaded nanomaterials with a diameter in the range of 10 to 200 nm are considered to be ideal nanomedicines for rational use of the EPR effect for passive targeting.[25] In addition, surface modification and the charge of nano-drugs also play important roles in drug enrichment. Nanoparticles with a neutral or negative charge on their surface or modified with polyethylene glycol (PEG) are also conducive to their enrichment at tumor sites due to their extended blood circulation time, while positively charged nanoparticles have a stronger penetrating ability, which in turn increases their opportunity to enter tumor tissues.[26,27] Recent studies have proven that the EPR effect is much more complex than the original definition, which is related to dozens of biological features including vascular permeability, angiogenesis, hemodynamic regulation, and tumor heterogeneity, hindering the applications of chemotherapy based on nanomedicine. Moreover, even if nano-drugs can be enriched in tumors, achieving the specific and effective release of drugs and overcoming drug resistance of chemotherapy in the hypoxic TME are urgent issues to be solved.

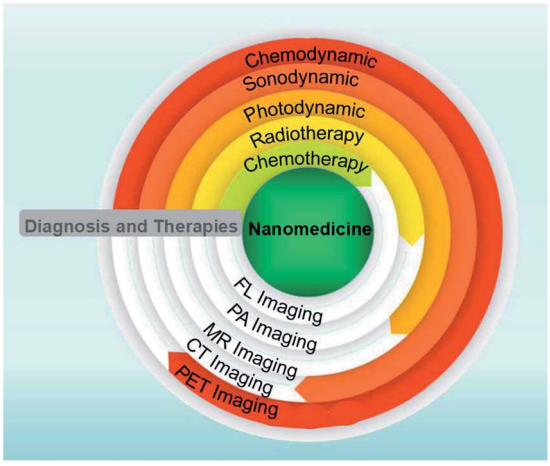

Fig. 2 Schematic illustration of the diagnosis and therapeutic applications of nanomedicines.

Because of the EPR effect and the discrepancy in pH between normal tissue and the TME, acid-responsive drug delivery nanosystems have been designed. Chen *et al.* fabricated a hybrid reduced graphene oxide-loaded ultrasmall Au nanorod vesicle (rGO-AuNRVe) (Fig. 3A).[29] According to the transmission electron microscopy (TEM) image, the vesicle was ~65 nm, which is suitable for passive targeting at tumor sites (Fig. 3B). Notably, the vesicle exhibited an accelerated drug release (DOX) performance (Fig. 3C) by utilizing acidity and laser-converted heat, which resulted from the reduction in the electrostatic interaction between DOX and the nanocarrier. Besides stimulating the release of DOX, the light absorption characteristic of rGO-AuNRVe gives it PAI and photothermal imaging capabilities, which have advantages such as high optical resolution and deep penetration depth, and real-time detection of the temperature at the tumor site (Fig. 3D and E), respectively. Furthermore, positron emission tomography (PET) imaging was used to detect the distribution of rGO-AuNRVe due to its high sensitivity, which can be used as a whole-body screening to identify specific areas.[28] The PET imaging results exhibited that there was ~9.7% ID g^{-1} of the ^{64}Cu-labeled hybrid vesicles in the tumor tissue after 24 h. This high local content of nanomedicine in the tumor site resulted from the EPR effect, and thus TME-responsive drug release is beneficial to enhance the therapeutic efficacy.[29]

Due to the fact that the passive targeting effect of the EPR effect is greatly affected by various factors of the complex TME, some nanomedicines based on active targeting have emerged. Active targeting methods rely on certain tumor biomarkers to achieve tumor targeting, which is achieved by loading active targeting groups or molecules onto a nanomedicine to specifically combine with the over-expressed receptors on tumor cells. Commonly used targeting molecules or groups mainly include antibodies (anti-CD44 monoclonal antibody and antitissue factor antibody fragment), transferrin (Tf), folic acid (FA), peptide (arginine–glycine–aspartic acid (RGD) tripeptide) and nucleic acid aptamers. Currently, dual active targeted therapies have also been developed to improve treatment outcomes. For instance, Jiang *et al.* developed a new vasculature and circulating tumor cell dual-targeted delivery system to enhance the chemotherapeutic efficacy of PTX, in which the K237 peptide and Ep23 aptamer can target tumor vessels and epithelial cell adhesion molecules on the surface of circulating tumor cells. Due to the combination effects of the dual active targeting strategy, the drug-loaded nanoparticles show enhanced cellular uptake and cytotoxicity. *In vivo* studies have shown that nanodrugs with dual targeting function achieve better therapeutic efficacy in tumor-bearing mice compared with unmodified or single-targeted nanoparticles.[30]

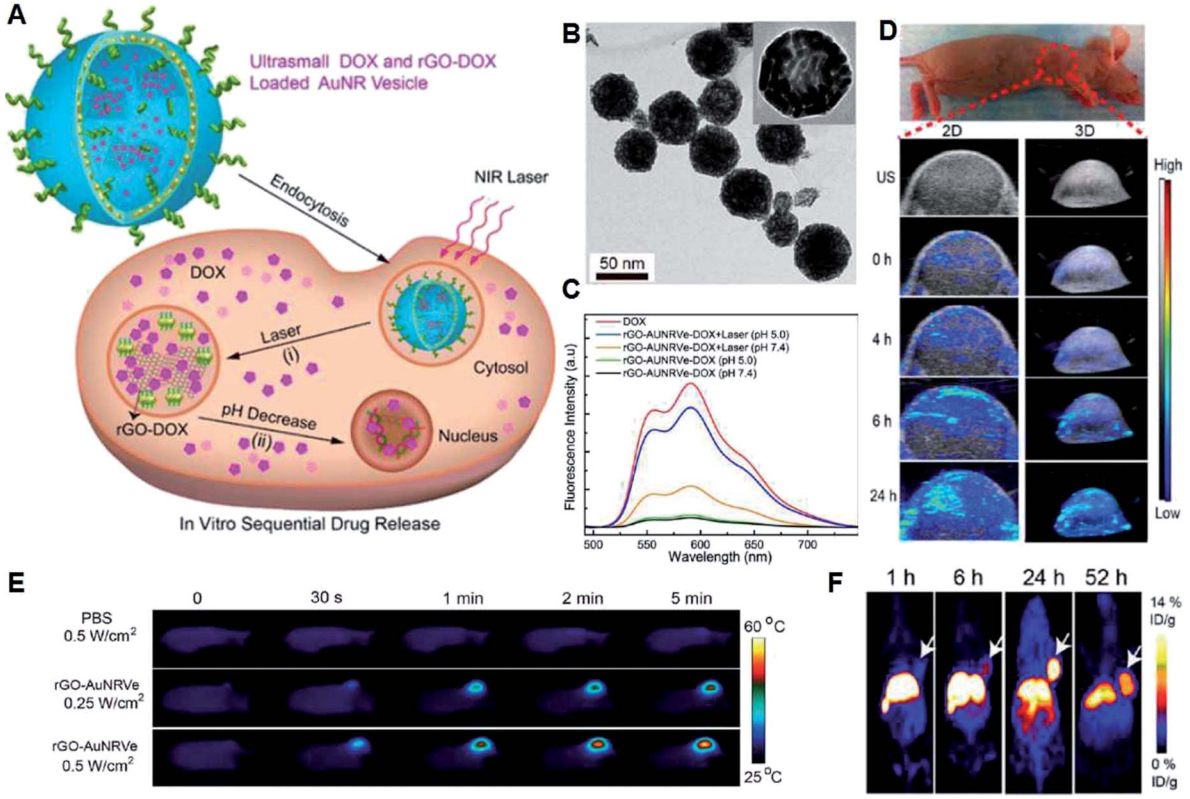

Fig. 3 (A) Release of DOX stimulated by photothermal effect and acidity. (B) TEM image of rGO-AuNRVe. (C) FL spectra of DOX and rGOAuNRVe-DOX treated with or without NIR laser illumination at pH 7.4 or pH 5.5. (D) *In vivo* ultrasound (US) PAI of the tumor region after intravenous administration of rGO-AuNRVe at 0, 4, 6 and 24 h. (E) Thermal imaging of the mice irradiated by 808 nm laser (0.25 W cm^{-2} or 0.5 W cm^{-2}) after the injection of different solutions. (F) Decay-corrected whole-body PET images of mice at different time points after intravenous injection of [^{64}Cu]-labeled rGO-AuNRVe (150 μCi).[29]

Besides increasing the tumor enrichment and release of drugs, solid tumors with hypoxic regions often limit the efficiency of chemotherapy.[14,31] Consequently, chemotherapy and oxygen-generation nanoplatforms were designed. Cai *et al.* developed a cancer cell membrane camouflaged nanocarrier encapsulated with DOX and hemoglobin (Hb) for chemotherapy (Fig. 4A), and the prepared DHCNPs could realize the homologous targeting of cancer cell adhesion molecules and oxygen-transporting abilities of Hb for O_2-enhanced chemotherapy (Fig. 4B).[32] According to the TEM image, the DHCNPs exhibit an obvious core–shell structure with a size of ~50 nm (Fig. 4C), and the absorption peaks of Hb and DOX in DHCNPs are consistent with free Hb and DOX molecules in the UV-Vis absorption spectra (Fig. 4D), demonstrating the successful loading of Hb and DOX. Benefitting from the increased O_2, the chemoresistance induced by hypoxia was broken through down-regulation of the expression of hypoxia inducible factor 1α (HIF-1α), multidrug resistance gene 1 (MDR1) and P-glycoprotein (P-gp) in cancer cells (Fig. 4E–G), leading to an enhancement in the effectiveness of DOX in the hypoxic TME. Furthermore, fluorescence (FL) imaging of DOX was used to measure the distribution of DHCNPs at 24 h post intravenous administration (Fig. 4H). The DCNPs and DHCNPs escaped from renal clearance with reduced FL signals of DOX in the kidneys, which can be attributed to the camouflage of the cancer cell membrane. In addition, since PAI can use endogenous contrast agents (such as hemoglobin, lipids, melanin, and water) to provide information on the structure, function, molecular and dynamics of deep tissue and the absorption between oxygenated hemoglobin (HbO_2) and deoxygenated Hb is different, the tumor oxygenation was assessed by PAI. It was found that the PA signal of HbO_2 was significantly enhanced in the surrounding blood vessels within 12 h after intravenous injection of DHCNPs (Fig. 4I), which demonstrates that DHCNPs relieved the hypoxic TME through the homologous targeting and oxygen self-supplying abilities of DHCNPs. Thus, this study proves that loading hemoglobin into a nanomedicine can indeed solve tumor hypoxia and enhance the effect of chemotherapy.

To date, *in vivo* experiments of chemotherapeutic nanomedicines mainly focused on subcutaneous tumor models. However, there is a need for systematic studies on the effects of these nanomedicines in metastatic tumor models, *in situ* tumor models and drug-resistant tumor models, which will aid in the evaluation of clinical translations. Furthermore, the establishment of new methods for the comparison of the curative results of different drugs will facilitate the selection of clinical nanomedicines. We believe that an increasing amount of intelligent

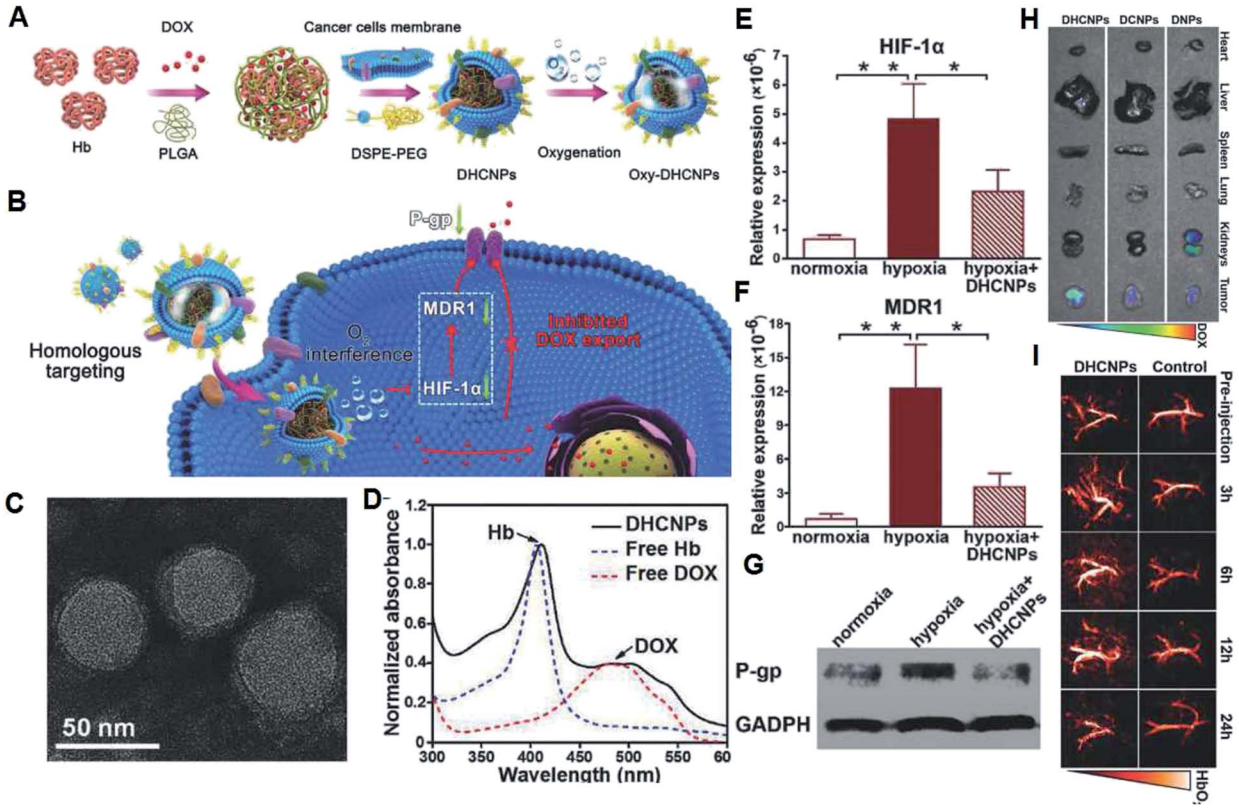

Fig. 4 (A) Synthesis of oxy-DHCNPs. (B) Schematic illustration of the therapeutic mechanisms of DHCNPs. (C) TEM image of DHCNPs. (D) UV-Vis absorption spectra of different solutions. (E–G) Contents of HIF-1α, MDR1, and P-gp of MCF-7 cells treated with DHCNPs. (H) FL images of normal organs and tumors of tumor-bearing mice after injection of different solutions. (I) PA images of tumors after the injection of DHCNPs.[32]

nanomedicines that are responsive to the TME will reach the clinical stage for targeted chemotherapy of various malignant tumors in the near future.

3. Enhanced radiotheranostics by regulating the TME

Radiation therapy (RT) is one of the primary tumor therapeutic patterns in the clinical treatments *via* one or more types of ionizing radiation.[33,34] Radiotherapy mainly includes external beam radiation therapy (EBRT) and internal radioisotope therapy (RIT). However, due to the low absorption of ionizing radiation by tumors, high doses of ionizing radiation are often used during RT, which may cause serious damage to normal tissues. With the development of nanotechnology, new nanomedicines that can enhance the radiation response in TME have attracted widespread attention, such as nanomaterials that contain components of elements with a high atomic number (*Z* number), which can act as radiosensitizers and absorb radiation (such as X-rays).[34] For example, Chen *et al.* reported a new generation of radiosensitizers based on Bi_2Se_3 NPs modified by polyvinylpyrrolidone and selenocysteine (PVP-Bi_2Se_3@Sec NPs), which can enhance the RT effect due to the high atomic number of the Bi element (Fig. 5). These PVP-Bi_2Se_3@Sec NPs are biodegradable and part of the selenium can be released and enter the blood circulation system, thereby enhancing the immunological function and reducing the side effects of whole body radiation. As a result, after the combination of RT and photothermal treatment with the materials based on the superior NIR absorption of Bi_2Se_3, PVP-Bi_2Se_3@Sec NPs achieved a simple but universal method to tumor treatment.

However, the unique inherent characteristics of many solid tumors are also key factors that limit the effectiveness of cancer radiotherapy, such as tumor invasion, metastasis, recurrence, and resistance to RT. For example, the efficiency of RT is subject to radiation resistance associated with tumor hypoxia.[33] Chen *et al.* fabricated core–shell nanoparticle-based poly(lactic-*co*-glycolic) acid (PLGA), where catalase (CAT) was encapsulated in the inner core, and imiquimod (R837) and toll-like-receptor-7 agonist were loaded in the PLGA shell (Fig. 6A). The final PLGA-R837@Cat NPs showed a spherical shape with a size of ~100 nm (Fig. 6B and C), and they could obviously increase the radiotherapy efficacy by relieving the hypoxic tumor (Fig. 6D and E) because the encapsulated CAT could decompose H_2O_2 to oxygen. Notably, the CAT in the core of PLGA-R837@Cat was well protected and ~60% of its original enzyme activity was maintained. As a result, the PLGA-R837@Cat NPs can enhance the therapeutic efficiency of radiotherapy.[35] This specific strategy of oxygen generation response to the TME with the help of natural catalase can be used as a universal method to

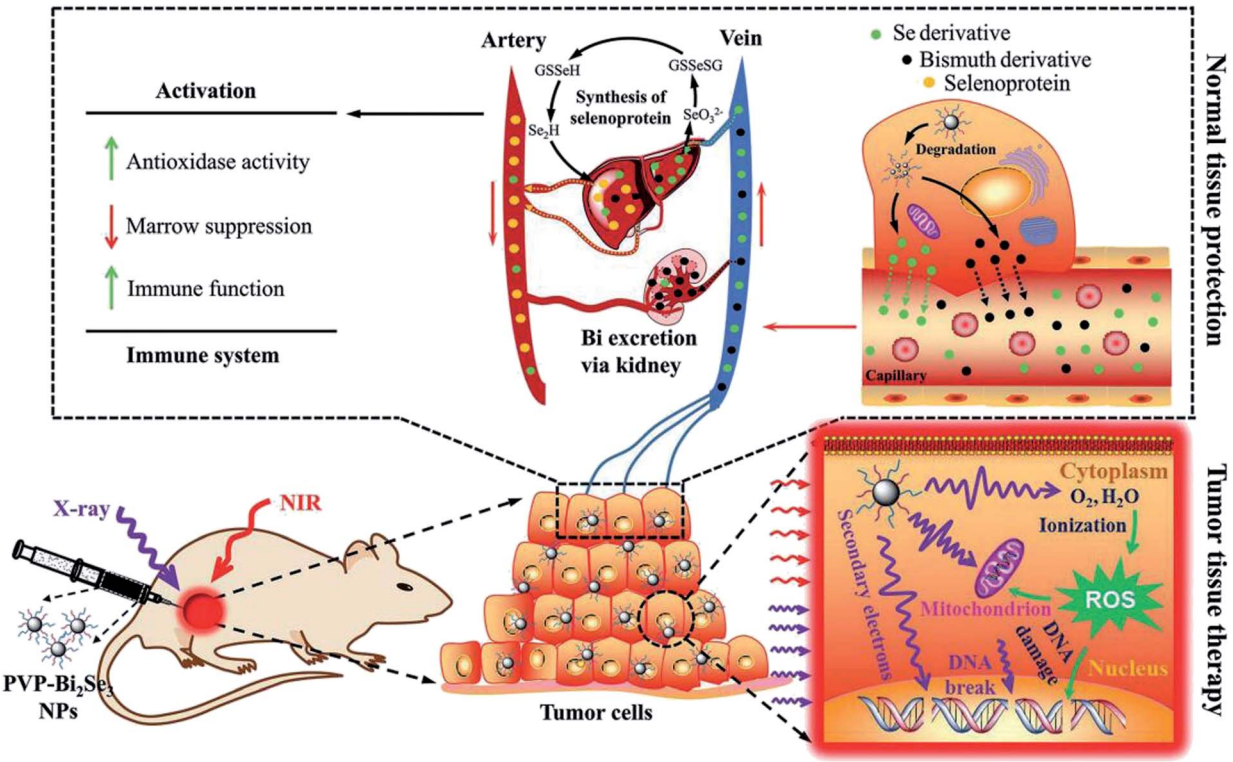

Fig. 5 Therapeutic mechanism of PVP-Bi_2Se_3@Sec NPs.[34]

overcome tumor hypoxia, which is of great significance not only in radiotherapy, but also other treatments.

Besides the *in situ* generation of oxygen, there are many oxygen carriers based on hemoglobin or perfluorocarbon (PFC). For example, PEG-polymerized bovine hemoglobin can be used to increase the tumor oxygen content and improve the curative effect of tumor radiotherapy. It has also achieved certain results in animal experiments.[36] PFC has excellent gas dissolving ability and can efficiently realize oxygen transportation.[37] Liu *et al.* prepared PEG-Bi_2Se_3@PFC NPs, which can serve as an oxygen reservoir and gradually release oxygen, offering an improved radio-sensitization effect at the *in vitro* level. The existence of Bi with a high *Z* number can synergistically enhance RT by radio-sensitization.[38]

In addition to alleviating tumor hypoxia, nanomedicines will bring new opportunities for RT by adjusting other parameters within the TME, such as lowering the pH of the tumor and normalizing the tumor vasculature. However, designing and preparing new nanomedicines for targeting new parameters within the TME are still current challenges.

4. Enhanced photodynamic theranostic by regulating TME

In addition to the above mentioned traditional chemotherapy and radiotherapy, researchers are focusing on new therapies based on nanomedicine. Accordingly, photodynamic therapy (PDT) is one type treatment that uses exogenously generated reactive oxygen species (ROS) produced by photosensitizers (PSs) through photoactivation to kill cancer cells.[39–42] PDT typically involves three main components, a specific light source that can provide power to a specific photodynamic reaction; PS that can collect this light and perform a photodynamic reaction; and an oxygen-containing substrate (such as molecular oxygen, water). This therapy is non-invasive and will not damage normal cells due to the selective illumination. Many organic PSs including chlorin e6 (Ce6), methylene blue (MB) and indocyanine green (ICG) mainly produce singlet oxygen ($^1O_2$) through the oxygen-dependent type II PDT (energy transfer) process.[43] Specific PSs can also generate superoxide anion ($^{\bullet}O_2^-$) and hydroxyl ($^{\bullet}OH$) radicals through the type I PDT (electron transfer) process.[44,45] However, traditional PDT faces several challenges, including light-dependent activation, light penetration depth, PS and O_2 dependence, PS enrichment and over-expressed GSH.[46] The latest advances in nanotechnology provide a common platform for the development of PDT and many nanomaterials after sensible optimization that can increase the content of oxygen or reduce the content of GSH in TME have been prepared.[47]

In our group, we prepared many TME-responsive PDT nanoagents for effective tumor therapy. Specifically, we used a one-step biomineralization method to prepare bovine serum albumin–iridium oxide nanoparticles (BSA–IrO_2 NPs) (Fig. 7A) with CAT-like activity (Fig. 7B), photocatalytic activity (Fig. 7C) and high photothermal conversion efficiency (η = 67.8%) (Fig. 7D), which can realize efficient photothermal therapy and self-enhanced photodynamic therapy. Furthermore, the high X-ray absorption coefficient of Ir allows effective CT imaging with

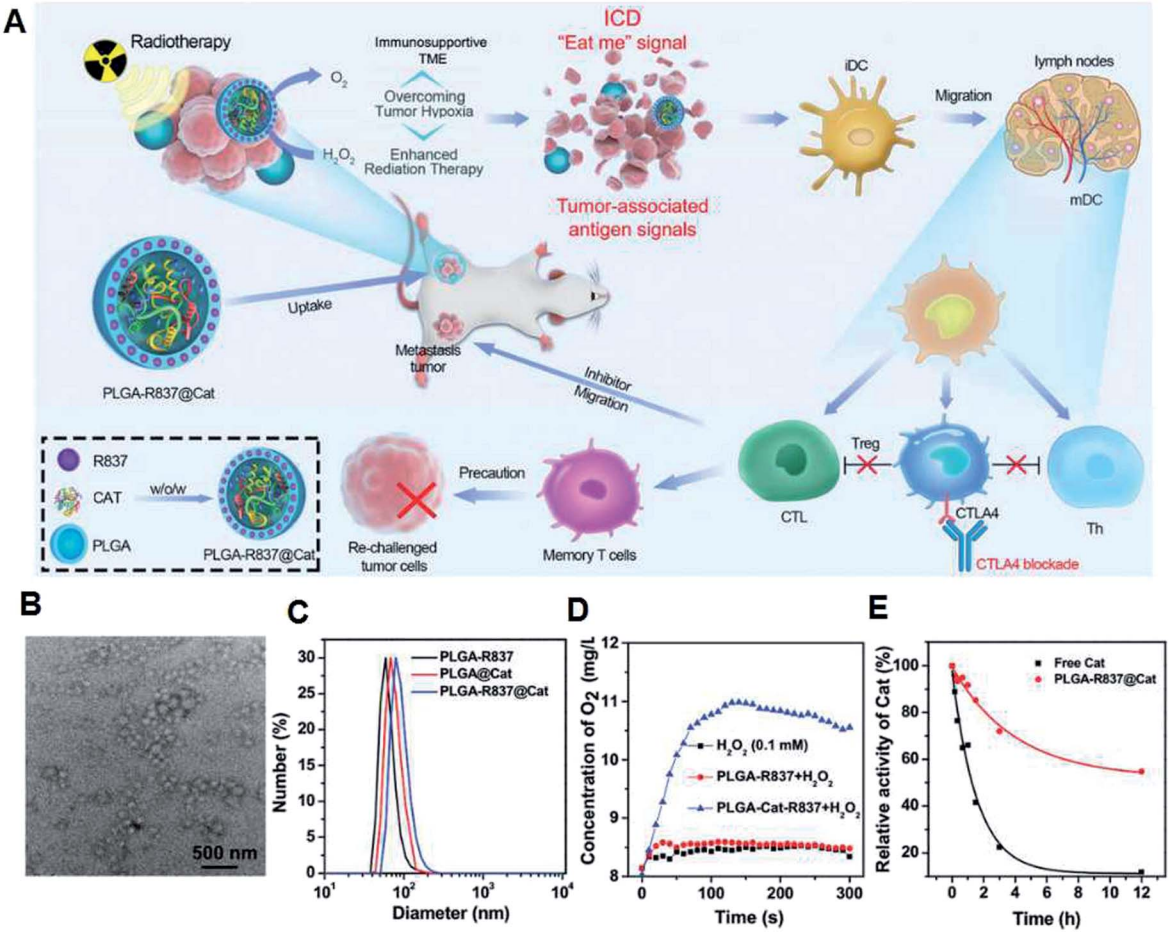

Fig. 6 (A) Therapeutic mechanism of PLGA-R837@Cat. (B) TEM image of PLGA-R837@Cat NPs. (C) Hydrodynamic diameter of different solutions. (D) Generation of O_2 in H_2O_2 solution (0.1 mM) with PLGA-R837 or PLGA-R837@Cat. (E) CAT activities of free CAT molecule and PLGA-R837@Cat NPs with same content of CAT after the digestion of protease K for different periods.[35]

deep-tissue penetration (Fig. 7E), together with high spatial resolution in soft tissues for PA imaging resulting from the effective photothermal effect (Fig. 7F), and thus the BSA–IrO_2 NPs can act as an effective nanomedicine for tumor theranostics.[48] We also prepared novel dihydroartemisinin (DHA) and methylene blue (MB) co-loaded Fe-doped polydiaminopyridine nanofusiforms (Fe-PDAP NFs) (Fig. 8A and B) for the decomposition of H_2O_2 to O_2, and the generated O_2 can enhance PDT (Fig. 8C). The Fe-PDAP NFs can also consume GSH (Fig. 8D) and release Fe^{2+} for further increasing the toxicity of DHA (Fig. 8E). Furthermore, due to the presence of Fe, they can be used for MR imaging to monitor tumor phototherapy with high-resolution in soft tissues (Fig. 8E–G).[49] Both of these nanomedicines achieved the integration of diagnosis and oxygen generation through their catalase-like activity to enhance photodynamic therapy, and thus have great prospects for clinical transformation.

Since light is the energy source for PDT, the penetration depth and transmission efficiency of light are still obstacles for deep cancer treatment because light can be significantly reflected and decayed when it interacts with tissues (such as the skin). Thus, to overcome the limited penetration depth of lasers, there are several strategies. The first is to use up-conversion nanoparticles (UCNPs) or two-photon-excited nanoparticles as light sensors to absorb light in the NIR region and emit it in the visible region, thereby exciting nearby PS molecules.[50,51] The second strategy is to use X-rays with a deeper tissue penetration depth as the light source. This strategy uses nano-scintillators to convert X-rays into visible light, and then activates nearby PS molecules.[52] The third method is to *in situ* generate fluorescence and achieve endogenous activation of PS molecules by bioluminescence resonance energy transfer (BRET) systems combining the bioluminescent luciferase and quantum dots.[53] The fourth is the use of Cherenkov radiation, where when high-speed charged particles move faster than the speed of light in the medium, they can emit visible light (250–600 nm) and excite nearby PS molecules.[54]

Although the mechanism of PDT is clear and many ideal nanomedicines with oxygen generation and absorption peaks in the range of 700 to 1100 nm were explored to allow deep tissue penetration and PDT drugs have also been approved for clinical use, PDT has not yet been accepted as a first-line treatment

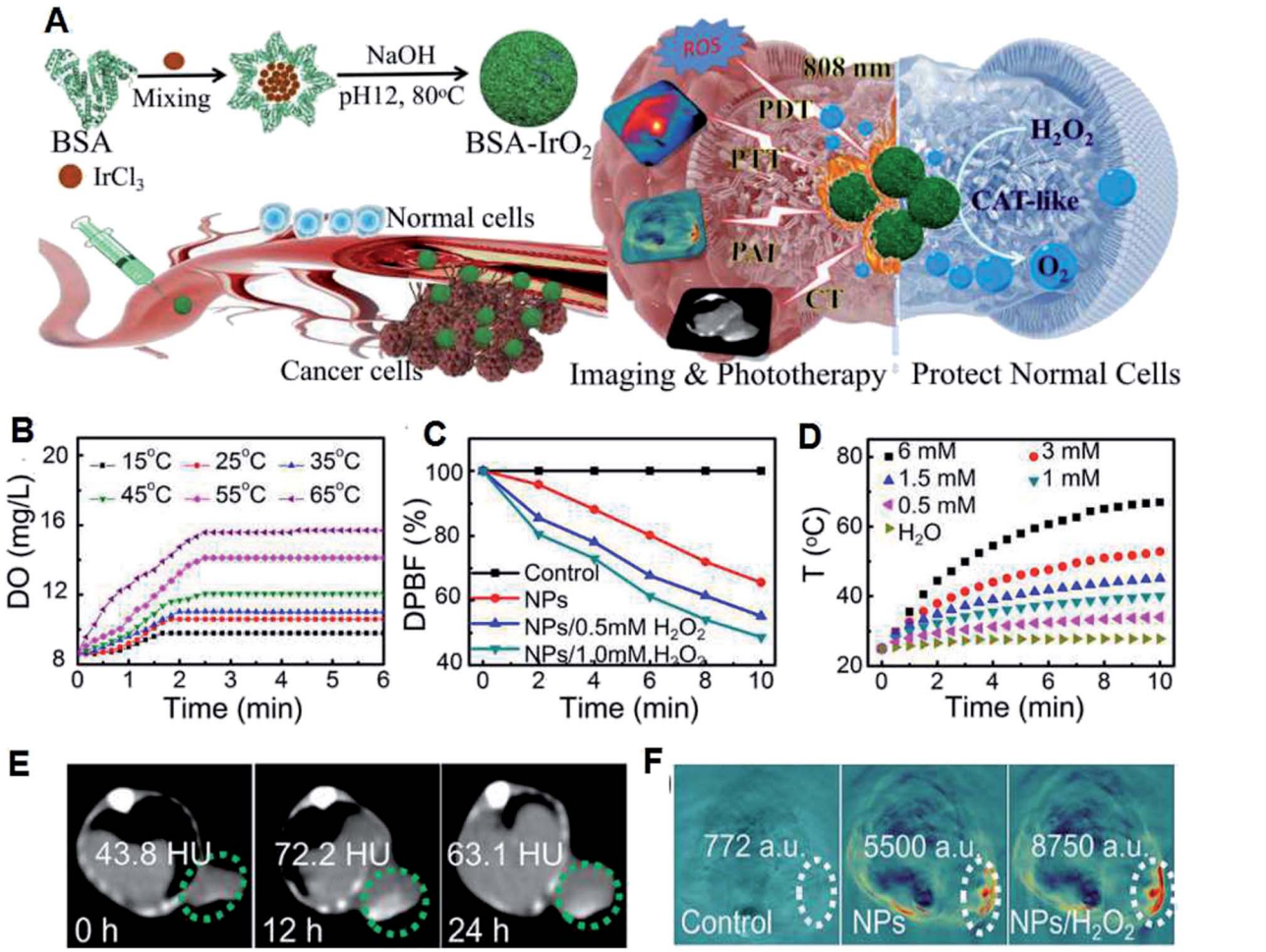

Fig. 7 (A) Preparation and the therapeutic mechanism of BSA–IrO_2 NPs. (B) Temperature-dependent H_2O_2-triggered O_2 generation by BSA–IrO_2 aqueous solution (DO: dissolved oxygen). (C) Generation of ROS evaluated by DPBF under irradiation. (D) Photothermal effect of BSA–IrO_2 with different contents of Ir. Mice pre- and post-intravenous administration of BSA–IrO_2 NPs for (E) CT imaging at different time points and (F) PA imaging at 12 h or further treatment with H_2O_2.[48]

option. Additionally, transforming PDT into clinical practice also is a challenge.

5. Enhanced sonodynamic theranostic by regulating the TME

Recently, due to the restricted penetration of light[55] in PDT, ultrasound (US)-triggered sonodynamic therapy (SDT) with deep penetration in biological tissues has developed quickly.[56,57] However, although it has been widely proven that SDT can produce ROS and realize further anti-tumor effects, its precise treatment mechanism is still unclear. The currently accepted explanation is that ultrasound cavitation can cause sonoluminescence or pyrolysis, which may be beneficial for the production of ROS by sonosensitizers. The so-called cavitation effect refers to the generation of bubbles after ultrasound irradiation, and cavitation is the rapid growth and collapse of bubbles. It is more interesting to find that ultrasound can also activate traditional sonosensitizer molecules (such as hematoporphyrin) to produce ROS through perforation, sonochemistry, and sonoluminescence, and then kill cancer cells. However, the low bioavailability and instability of traditional organic sonosensitizers[58–61] and tumor hypoxia greatly limit the efficiency of SDT and its prospective clinical use.[62,63]

To solve the above problems, different oxygen-generating nanomedicines have been constructed based on titanium dioxide, some metal–organic frameworks (MOFs) and organic PS molecule-loaded nanomaterials. Shi *et al.* successfully developed multi-functional PMR nanosonosensitizers through the combination of MnO_x with hollow mesoporous organosilica NPs, followed by its integration with protoporphyrin (sonosensitizer) and cyclic arginine–glycine–aspartic pentapeptide (targeting peptide) (Fig. 9A and B). MnO_x acts as an inorganic catalase-like nanozyme for consuming the over-expressed H_2O_2 in the TME to generate oxygen (Fig. 9C and D), which contributes to a decrease in the expression level of HIF-1α (Fig. 9E). The generated oxygen can facilitate the production of $^1O_2$ induced by SDT as abundant oxygen (Fig. 9F).[64] In addition, PAI was used to analyze the variation in oxygen concentration due to the different absorptions of HbO_2 and Hb.[52] It is obvious that the PA

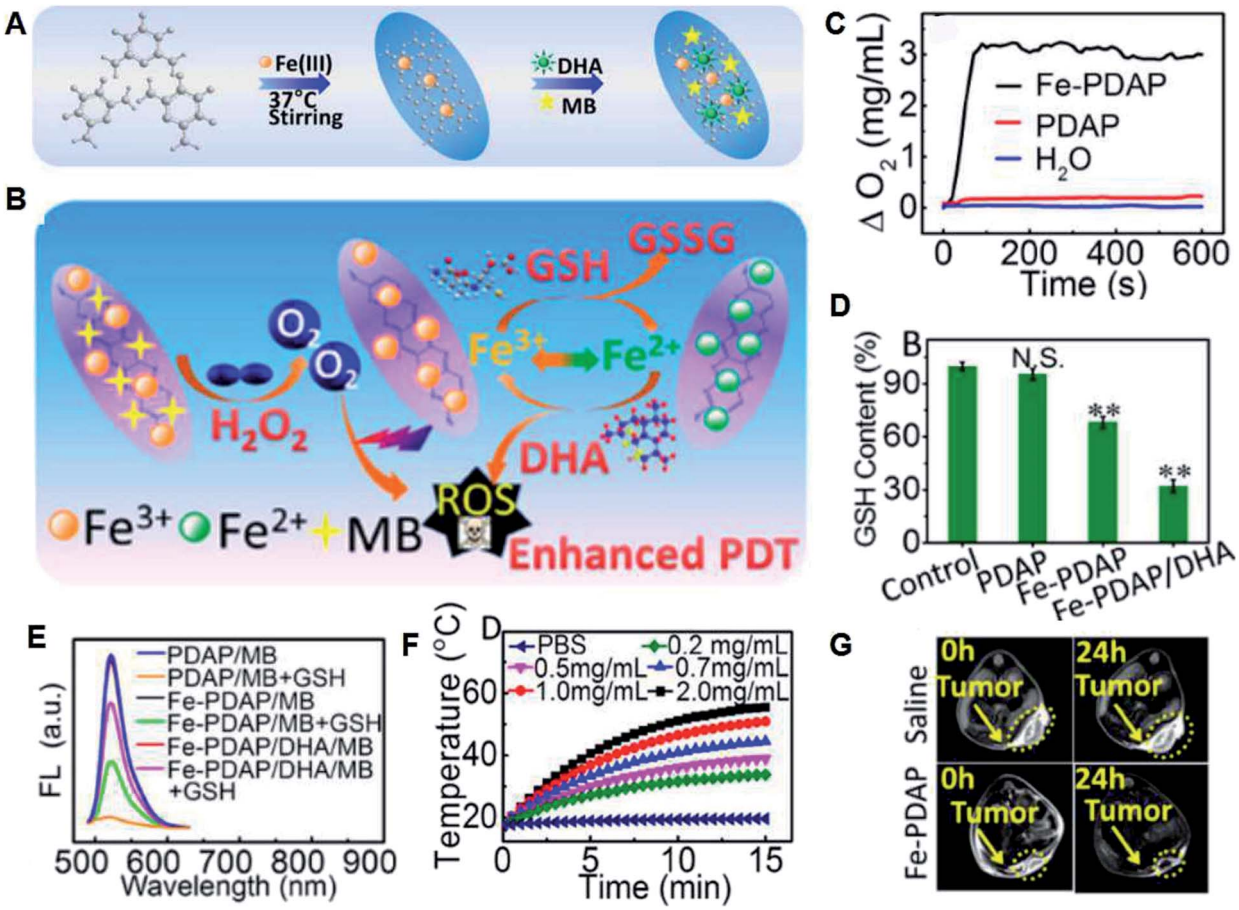

Fig. 8 (A) Synthesis of Fe-PDAP NFs and further loading of MB and DHA. (B) Therapeutic mechanism of MB/DHA-loaded Fe-PDAP NFs. (C) H_2O_2-triggered O_2 production in different solutions. (D) Intracellular contents of GSH incubated with different agents. (E) Generation of $^1O_2$ measured by the fluorescence of DCFH. (F) Photothermal effect of Fe-PDAP NFs with different concentrations. (G) *In vivo* MRI of tumor-bearing mice at 24 h post-injection of different solutions.[49]

signal was enhanced after the administration of the PMR nanosonosensitizers (Fig. 9G), demonstrating the effective CAT-like activity of MnO_x in TME oxygenation. Moreover, the released Mn^{2+} at the specific TME (GSH and mild acidity) and the obvious brightening effect in the T_1-weighted MRI of the tumor tissue after the intravenous administration of the nanomedicine provide more information about tumor diagnosis. Overall, PMR nanosonosensitizers can effectively enter tumor tissue through both the EPR effect and RGD targeting, and can be used for self-enhanced SDT and PA/MR imaging.

As a new cancer treatment method, SDT is still in its infancy, but although it shows broad application prospects and room for development, there are many problems that need to be solved, including accurate therapeutic mechanisms, how to further improve the efficiency of SDT, and how to expand the scope of the applications of SDT.

6. Enhanced chemodynamic theranostic by regulating the TME

PDT and SDT need an exogenous energy input including light or ultrasound,[65,66] which may not collect the desired pathological changes in tissue due to the limitations of penetration depth or rapid energy decay. Thus, a new therapy that can also generate ROS without additional energy, including light, ionizing irradiation and ultrasound while triggered by endogenous chemical energy is attractive and is called chemodynamic therapy (CDT).[67,68] CDT often takes advantages of Fenton reactions mediated by two/three-valence ions, Fe^{2+} and Fe^{3+}. Fenton reactions can produce the most toxic $^{\cdot}OH$ in cancer cells by catalyzing over-produced H_2O_2 in the mildly acidic TME. Accordingly, many Fe^{2+}/Fe^{3+}-based nanocatalysts including Fe^{2+}/Fe^{3+}-loaded or selectively Fe^{2+}/Fe^{3+} released nanoparticles have been developed to activate *in situ* Fenton reactions.[69–71] Focusing on modulating the reaction environment of CDT, Shi *et al.* prepared a sequential catalytic nanomedicine for effective tumor treatment by co-loading the natural glucose oxidase (GOx) and ultrasmall iron oxide (Fe_3O_4) nanoparticles into the mesopores of dendritic silica nanoparticles, and the prepared nanomedicine was designated as GFD nanocatalysts (Fig. 10).[72] GOx is able to consume glucose and oxygen to generate gluconic acid and more H_2O_2 in tumor cells, which can enhance the Fenton reaction catalyzed by Fe_3O_4 NPs since the mildly acidic pH value of the TME and the concentration of H_2O_2 will also

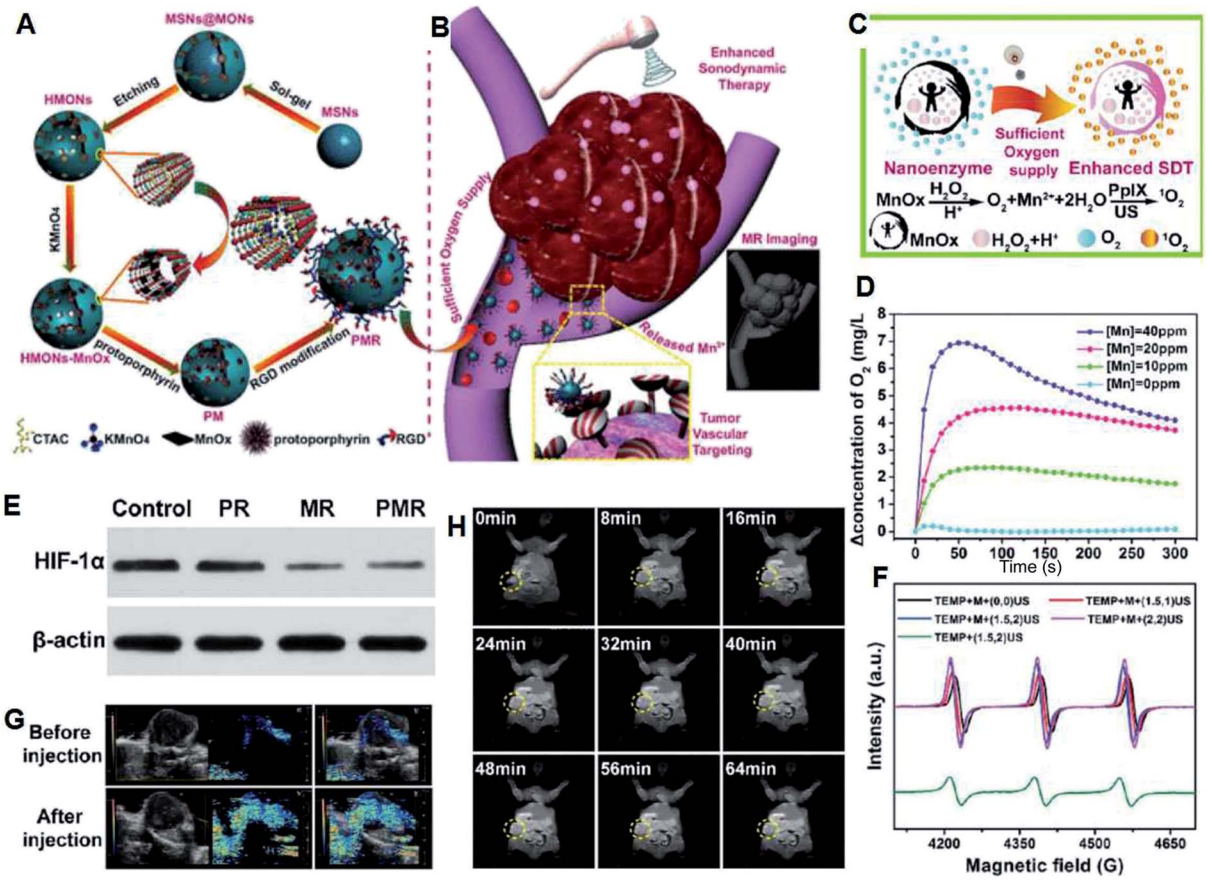

Fig. 9 (A) Synthesis and (B) therapeutic mechanisms of PMR sonosensitizers. (C) Schematic illustration of the production of O_2 and $^1O_2$ under US irradiation. (D) Generation of O_2 with different concentrations of Mn and H_2O_2 at different pH (6.5, 7.4). (E) HIF-1α expression levels at different groups demonstrated by western blot technique. (F) ESR spectra trapped by TEMP under different treatments. (G) Tumor oxygenation status as determined by *in vivo* PA imaging ([Mn] = 1 mg kg^{-1}). (H) T_1-Weighted MR imaging of mice after intravenous injection at different time points.[64]

limit the effect of CDT. Highly toxic $^{\bullet}OH$ is produced through the abovementioned sequential catalytic reactions and it can result in damage to tumor tissue. This work demonstrated that catalytic nanomedicines can attain therapeutic selectivity and efficiency by regulating the TME.[72]

Recently, several other ion, including Mn^{2+}, Co^{2+}, and Cu^{2+}, loaded and metal-based CDT nanoagents with Fenton-like reactions have also been used for CDT.[73–77] However, the overexpression of GSH is also one of the obstacles for CDT. Aiming at solving this restriction, several nanomaterials with GSH-consumption ability have been developed and used for tumor theranostics.[78–81] Li *et al.* prepared copper–amino acid mercaptide NPs (Cu–Cys NPs) with GSH-triggered and H_2O_2-enhanced CDT abilities for resisting breast tumors (Fig. 11A and B).[77] Firstly, the Cu–Cys NPs consume local GSH and reduce Cu^{2+} (Fig. 11C) to Cu^{+} (Fig. 11D and E). Afterwards, the H_2O_2 in the weakly acidic TME can react with the produced Cu^{+} to produce $^{\bullet}OH$ through a Fenton-like reaction (Fig. 11F), which contributes to the effective apoptosis of tumor cells.

In addition to the typical Fenton and Fenton-like reactions for the generation of ROS, the Russel mechanism is another interesting approach for CDT. Iron oxide NPs were integrated with linoleic acid hydroperoxide (LAHP), and the formed IO-LAHP was used for the *in situ* production of $^1O_2$. Therein, LAHP is related to the main product of lipid peroxidation, and certain H_2O_2 in lipids can be decomposed into radicals and $^1O_2$ by the Russel mechanism triggered by certain catalytic ions (such as Fe^{2+} and Ce^{4+}). IO-LAHP can slowly release Fe^{2+} under the mildly acidic TME, which further triggers LAHP to produce $^1O_2$, thereby greatly inhibiting the growth of tumors.[82] Recently, our group developed two-dimensional Cu–TCPP (tetrakis(4-carboxyphenyl)porphyrin) nanosheets (Fig. 12A and B), which can produce $^1O_2$ in the specific TME (Fig. 12C) based on the peroxidation of the TCPP ligand by acidic H_2O_2 followed by its reduction to peroxyl radicals (Fig. 12D) under the action of peroxidase (POD)-like Cu–TCPP and Cu^{2+} and their spontaneous recombination reaction triggered by the Russell mechanism (Fig. 12A). In addition, Cu–TCPP can also consume GSH and resist its protection effect against ROS (Fig. 12E). Consequently, Cu–TCPP can specifically and effectively destroy tumors, demonstrating an attractive approach for CDT (Fig. 12F and G).[83] Importantly, these nanomedicines with the Russell mechanism can generate singlet oxygen triggered by acidic pH without the need for external stimulation (laser and ultrasound), which provide a new strategy for tumor-specific treatment. However, this treatment method relies heavily on

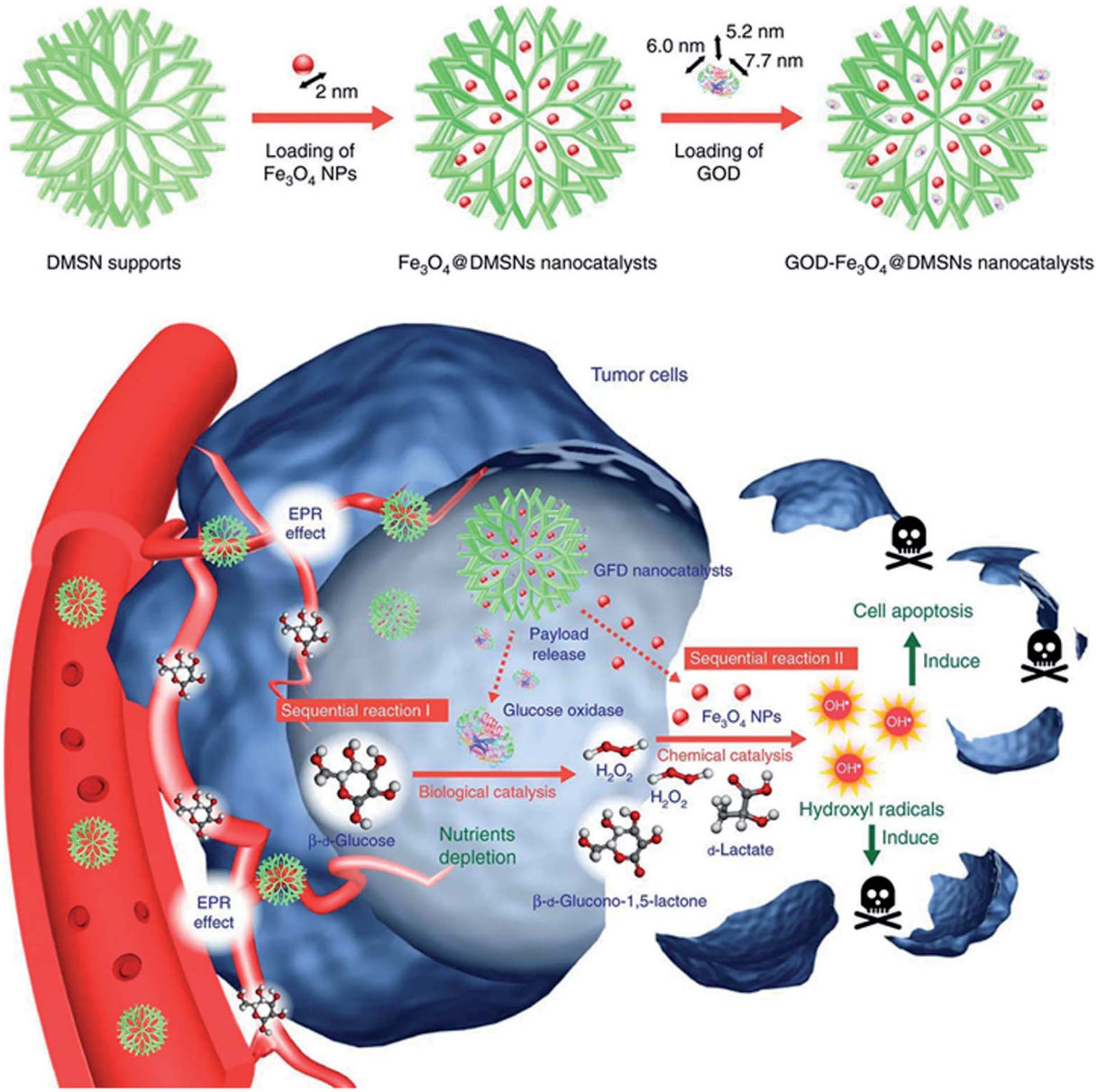

Fig. 10 Preparation and therapeutic mechanisms of GFD NCs.[72]

peroxygen bridges and the reaction mechanism is self-consumption, thus increasing the enrichment of the nanomedicine at the tumor site is the key issue.

CDT has become a "green" type of therapy with selectivity and specificity, which combines the characteristics of the TME with classic Fenton/Fenton-like reactions or the Russel mechanism to *in situ* destroy tumors, providing great potential for clinical translation.

7. Summary

The rapid development of nanotechnology and nanomedicine has promoted the emergence of many subdisciplines of biomedicine. Nanomedicine based on TME-triggered *in situ* chemical reactions is one of the recently emerging research fields, showing a wide range of potential and prospects for cancer theranostics. This minireview discusses the recent advances in the design and synthesis of biocompatible nanomedicines that are not only used to catalyze or trigger chemical reactions in the TME (including oxygen generation, acid-generation, glutathione consumption and production of ROS), but also have outstanding multi-model imaging (including PAI, CT imaging, MRI, PET imaging and thermal imaging) and tumor-specific treatment effects (including tumor chemotherapy, radiotherapy, photodynamic therapy, sonodynamic therapy and chemodynamic therapies). Nevertheless, the widespread application of TME-responsive nanomedicines is still in its infancy. It still needs further clinical translation to benefit patients because there are several key issues and challenges that need to be resolved before entering the preclinical stage, which will be explained in detail below.

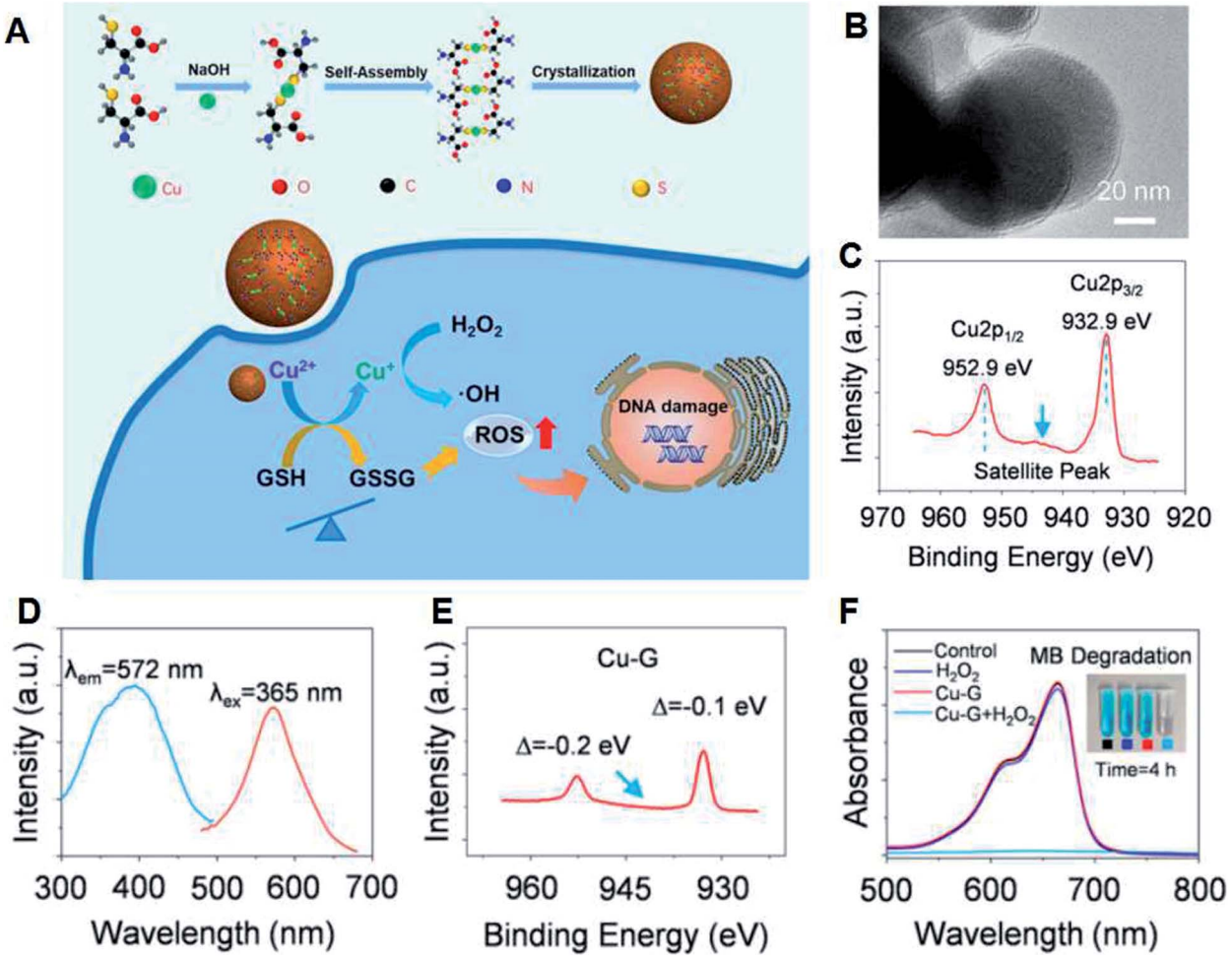

Fig. 11 (A) Synthesis and therapeutic mechanism of Cu–Cys NPs. (B) TEM image of Cu–Cys NPs. (C) Cu 2p XPS spectrum of the Cu–Cys NPs. (D) Excitation and emission spectra of Cu–Cys NPs reacted with GSH (Cu–G). (E) XPS spectrum of Cu–G. (F) MB degradation to demonstrate the generation of $^{\bullet}OH$.[77]

(1) Exploring new characteristics in the TME. The chemical reactions currently being explored for therapies are mainly based on exogenous physical triggers or commonly referred characteristics of the endogenous TME. However, the explored features of the TME with effective responses are still very limited. Therefore, there is a great need to develop new chemical reactions that are responsive to new characteristics of the TME with improved biomedical efficacy. For example, the concentration of the often targeted endogenous reactants such as oxygen and H_2O_2 is usually too low to elicit a significant response, and there is a large number of other biological species that should be explored and potentially developed as new candidate reactants for chemical reactions within the TME.

(2) Revealing the *in vivo* chemical reaction mechanisms during treatment. Although it has been widely proven that introduced chemical reactions are effective against cancer, the corresponding mechanisms have not been fully revealed at the animal experimental level. As indicated, the TME is much more complicated than conventional *in vitro* reaction conditions, and the presence of various species in living tissue may have a significant impact on a specific chemical reaction. In addition, due to the complicated metabolism of living systems, the TME is in a continuous equilibrium state, which also makes it difficult to accurately characterize the reaction process.

(3) Exploring new characterization methods for *in vivo* detection of chemical reactions. The lack of characterization methods for *in situ* chemical reactions makes it is difficult to quantify the raw materials or products during *in vivo* chemical reactions. Most reported results are mainly based on the final *in vivo* treatment results, but there is still a lack of in-depth understanding of the mechanism at various steps. Therefore, more attention should be paid to the development of new technologies to reveal the *in vivo* reaction mechanisms in the future.

(4) Exploring new nanoplatforms with multiple imaging capabilities. Although we introduced several different imaging modes, each has its own advantages and disadvantages. PAI is a hybrid imaging mode that combines optical illumination and ultrasound (US) detection, and it overcomes the light scattering and low resolution of pure optical imaging, but the problem is

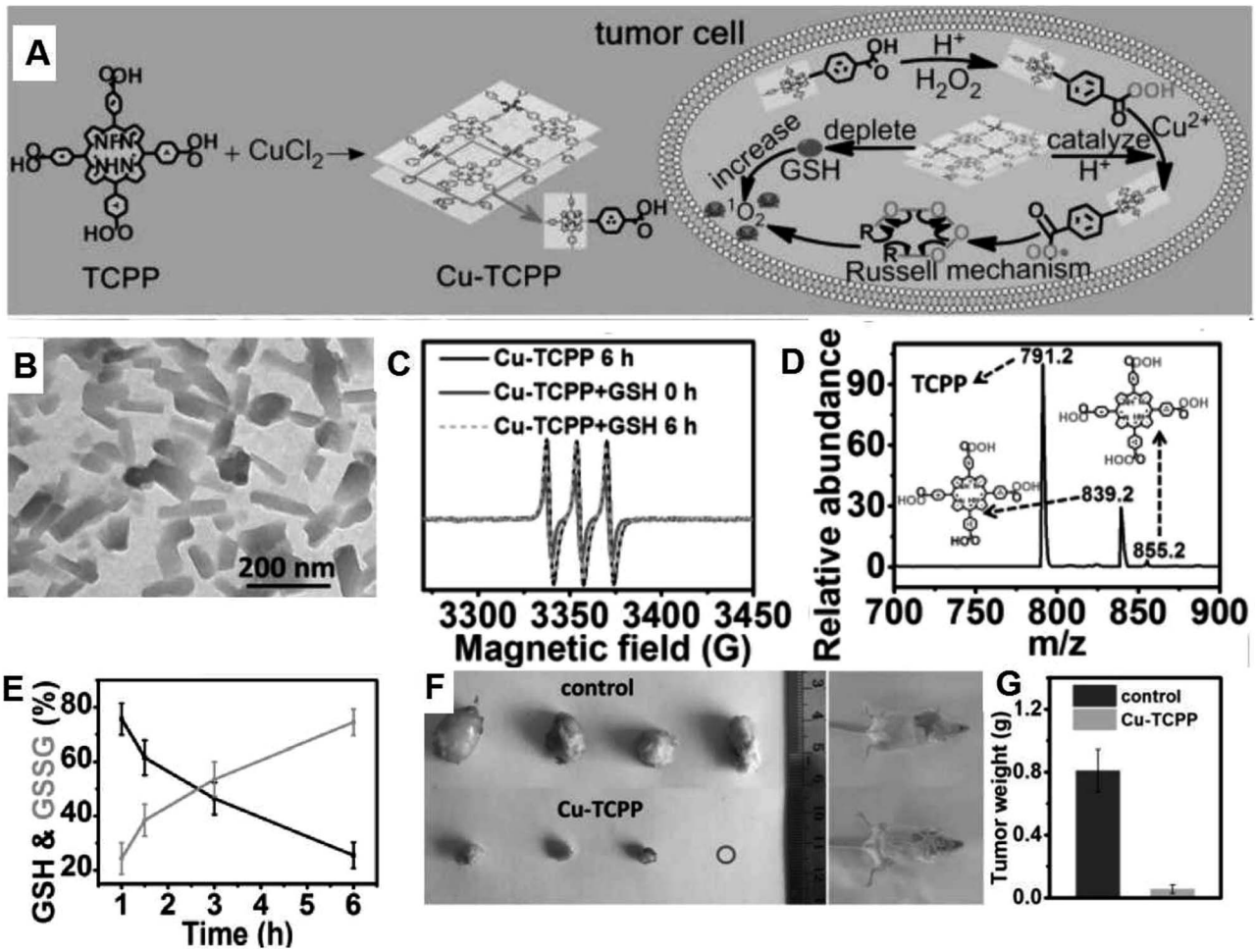

Fig. 12 (A) Synthesis and therapeutic mechanism of Cu–TCPP nanosheets. (B) TEM image of Cu–TCPP. (C) ESR spectra of Cu–TCPP with/without GSH upon the addition with TEMP and H_2O_2. (D) Mass spectrum of reaction solution including H_2O_2 and TCPP. (E) Variation in the ratio of GSH and GSSG in the supernatant of Cu–TCPP and GSH mixed solution at 1, 1.5, 3 and 6 h. (F) Photos of the tumors and mice after therapy. (G) Average weights of the tumors in the different groups.[83]

that the detection depth of PAI in the skin is only 10 mm, thus PAI still faces challenges in skin cancer detection. MRI has high-resolution of soft tissues, but its scan time is long. CT imaging has a quick scan speed, high sensitivity of hard tissue, deep-tissue penetration and can be used for radiation dose mapping, but its resolution of soft tissues is relatively low. PET imaging has high sensitivity and short scan time, and it can efficiently provide whole-body screening to identify specific areas, but it needs additional radio labels of ^{64}Cu, ^{111}In, ^{124}I, and ^{18}F. Thus, the combination of different imaging modes can overcome the respective shortcomings and provide more reliable information about diseases.

(5) In terms of technological development, combining different imaging modes into an integrated instrument system is significant. For example, in PAI, nanosecond-level pulsed lasers (pulse duration < 10 ns) are usually used to irradiate biological samples, and biomolecules can absorb light energy and convert it into heat, which causes photoacoustic signals. In MRI, the energy state of the hydrogen protons makes a difference upon the application of a radio frequency pulse. After the radio frequency pulse, the hydrogen protons return to their original energy state and the electromagnetic waves generated by resonance are emitted. The small differences in the nucleus vibrations between different pathological changes can be accurately detected by the three-dimensional image of the tissue after further computer processing. Thus, if an instrument is developed with both nanosecond-level pulsed lasers and an applied magnetic field (B_0), plus a powerful computer reconstruction system, it may be possible that two imaging modes can be achieved. Accordingly, the exploitation of new instruments with multi-imaging capacities will reduce time cost and improve the diagnostic accuracy and efficiency.

Finally, our goal is to find and design better nanomedicines with a combination of effective therapy and advanced diagnosis to provide specific, effective and safe methods to treat cancer based on the understanding of the differences between the TME and normal tissues. Thus, our review provides crucial insight for the future development of nanomedicines and will also stimulate interest in the exploration of new theranostic nanomedicines with good potential for future use.

Conflicts of interest

No conflicts to declare.

Acknowledgements

This work was financially supported by the Joint Sino-German Research Projects (21761132028), National Natural Science Foundation of China (21675149, 21874125, 21877107), the Key Research Program of Frontier Sciences, CAS (QYZDY-SSW-SLH019), and the Science and Technology Development Program of Jilin Province (20170414037GH, 20190201074JC, 20180101015JC), and K. C. Wong Education Foundation.

References

1 P. P. Yang, Q. Luo, G. B. Qi, Y. J. Gao, B. N. Li, J. P. Zhang, L. Wang and H. Wang, *Adv. Mater.*, 2017, **29**(15), 1605869.
2 M. Overchuk and G. Zheng, *Biomaterials*, 2018, **156**, 217–237.
3 R. A. Cairns, I. S. Harris and T. W. Mak, *Nat. Rev. Cancer*, 2011, **11**(2), 85–95.
4 K. Greish, Enhanced permeability and retention (EPR) effect for anticancer nanomedicine drug targeting, *Cancer Nanotechnology*, 2010, pp. 25–37.
5 Y. Qian, Y. Wang, F. Jia, Z. Wang, C. Yue, W. Zhang, Z. Hu and W. Wang, *Biomaterials*, 2019, **188**, 96–106.
6 S. Li, Y. Zhang, J. Wang, Y. Zhao, T. Ji, X. Zhao, Y. Ding, X. Zhao, R. Zhao, F. Li, X. Yang, S. Liu, Z. Liu, J. Lai, A. K. Whittaker, G. J. Anderson, J. Wei and G. Nie, *Nat. Biomed. Eng.*, 2017, **1**(8), 667–679.
7 H. Huang, S. Banerjee, K. Qiu, P. Zhang, O. Blacque, T. Malcomson, M. J. Paterson, G. J. Clarkson, M. Staniforth, V. G. Stavros, G. Gasser, H. Chao and P. J. Sadler, *Nat. Chem.*, 2019, **11**, 1041–1048.
8 V. Petrova, M. Annicchiarico-Petruzzelli, G. Melino and I. Amelio, *Oncogenesis*, 2018, **7**(1), 10.
9 Z. Yang, Y. Dai, L. Shan, Z. Shen, Z. Wang, B. C. Yung, O. Jacobson, Y. Liu, W. Tang, S. Wang, L. Lin, G. Niu, P. Huang and X. Chen, *Nanoscale Horiz.*, 2019, **4**(2), 426–433.
10 Z. Yang, W. Fan, W. Tang, Z. Shen, Y. Dai, J. Song, Z. Wang, Y. Liu, L. Lin, L. Shan, Y. Liu, O. Jacobson, P. Rong, W. Wang and X. Chen, *Angew. Chem., Int. Ed.*, 2018, **57**(43), 14101–14105.
11 W. Feng, X. Han, R. Wang, X. Gao, P. Hu, W. Yue, Y. Chen and J. Shi, *Adv. Mater.*, 2019, **31**(5), 1805919.
12 J. Jin, M. OvaisKim and C. Chen, *Nano Today*, 2018, **22**(18), 83–99.
13 D. Neri and C. T. Supuran, *Nat. Rev. Drug Discovery*, 2011, **10**(10), 767–777.
14 J. M. Brown and W. R. Wilson, *Nat. Rev. Cancer*, 2004, **4**(6), 437–447.
15 D. Hanahan and R. A. Weinberg, *Cell*, 2011, **144**(5), 646–674.
16 Q. Chen, C. Liang, X. Sun, J. Chen, Z. Yang, H. Zhao, L. Feng and Z. Liu, *Proc. Natl. Acad. Sci. U. S. A.*, 2017, **114**(21), 5343.
17 H. Lin, Y. Chen and J. Shi, *Chem. Soc. Rev.*, 2018, **47**(6), 1938–1958.
18 K. Fan, J. Xi, L. Fan, P. Wang, C. Zhu, Y. Tang, X. Xu, M. Liang, B. Jiang, X. Yan and L. Gao, *Nat. Commun.*, 2018, **9**(15), 1440.
19 P. Teodoro, C. Marta, G. A. Lgnacio and A. V. Ana, *Anticancer Res.*, 2009, **29**, 3957–3965.
20 X. Zhong, X. Wang, L. Cheng, Y. Tang, G. Zhan, F. Gong, R. Zhang, J. Hu, Z. Liu and X. Yang, *Adv. Funct. Mater.*, 2020, **30**(4), 1907954.
21 C. H. Yang, M. L. Kuo, J. C. Chen and Y. C. Chen, *Br. J. Cancer*, 1999, **81**(5), 796–799.
22 B. A. Arrick and C. F. Nathan, *Cancer Res.*, 1984, **44**(10), 4224.
23 M. Diehn, R. W. Cho, N. A. Lobo, T. Kalisky, M. J. Dorie, A. N. Kulp, D. Qian, J. S. Lam, L. E. Ailles, M. Wong, B. Joshua, M. J. Kaplan, I. Wapnir, F. M. Dirbas, G. Somlo, C. Garberoglio, B. Paz, J. Shen, S. K. Lau, S. R. Quake, J. M. Brown, I. L. Weissman and M. F. Clarke, *Nature*, 2009, **458**(7239), 780–783.
24 P. Ma, H. Xiao, C. Yu, J. Liu, Z. Cheng, H. Song, X. Zhang, C. Li, J. Wang, Z. Gu and J. Lin, *Nano Lett.*, 2017, **17**(2), 928–937.
25 S. Qin, A. Zhang and X. Zhang, *Small*, 2018, **14**, 1802417.
26 F. Alexis, E. Pridgen, L. K. Molnar and O. C. Farokhzad, *Mol. Pharmaceutics*, 2008, **5**(4), 505–515.
27 H. X. Wang, Z. Q. Zuo, J. Z. Du, Y. C. Wang, R. Sun, Z. T. Cao, X. D. Ye, J. L. Wang, K. W. Leong and J. Wang, *Nano Today*, 2016, **11**(2), 133–144.
28 X. Sun, X. Huang, X. Yan, Y. Wang, J. Guo, O. Jacobson, D. Liu, L. P. Szajek, W. Zhu, G. Niu, D. O. Kiesewetter, S. Sun and X. Chen, *ACS Nano*, 2014, **8**(8), 8438–8446.
29 J. Song, X. Yang, O. Jacobson, L. Lin, P. Huang, G. Niu, Q. Ma and X. Chen, *ACS Nano*, 2015, **9**(9), 9199–9209.
30 J. Yao, J. Feng, X. Gao, D. Wei, T. Kang, Q. Zhu, T. Jiang, X. Wei and J. Chen, *Biomaterials*, 2017, **113**, 1–17.
31 A. Persidis, *Nat. Biotechnol.*, 1999, **17**(1), 94–95.
32 H. Tian, Z. Luo, L. Liu, M. Zheng, Z. Chen, A. Ma, R. Liang, Z. Han, C. Lu and L. Cai, *Adv. Funct. Mater.*, 2017, **27**(38), 1703197.
33 S. M. Larson, J. A. Carrasquillo, N.-K. V. Cheung and O. W. Press, *Nat. Rev. Cancer*, 2015, **15**(6), 347–360.
34 J. Du, Z. Gu, L. Yan, Y. Yong, X. Yi, X. Zhang, J. Liu, R. Wu, C. Ge, C. Chen and Y. Zhao, *Adv. Mater.*, 2017, **29**, 1701268.
35 Q. Chen, J. Chen, Z. Yang, J. Xu, L. Xu, C. Liang, X. Han and Z. Liu, *Adv. Mater.*, 2019, **31**(10), 1802228.
36 R. Linberg, C. Conover, K. Shum and R. Shorr, *In Vivo*, 1997, **12**, 167.
37 L. Xu, X. Qiu, Y. Zhang, K. Cao, X. Zhao, J. Wu, Y. Hu and H. Guo, *J. Transl. Med.*, 2016, **14**, 268.
38 G. Song, C. Liang, X. Yi, Q. Zhao, L. Cheng, K. Yang and Z. Liu, *Adv. Mater.*, 2016, **28**(14), 2716–2723.
39 R. N. Kjellberg, *Science*, 1972, **176**, 1071.
40 B. Yang, Y. Chen and J. Shi, *Chem. Rev.*, 2019, **119**(8), 4881–4985.
41 X. Ma, Y. Wang, X.-L. Liu, H. Ma, G. Li, Y. Li, F. Gao, M. Peng, H. M. Fan and X.-J. Liang, *Nanoscale Horiz.*, 2019, **4**(6), 1450–1459.
42 H. Zhang, K. Liu, S. Li, X. Xin, S. Yuan, G. Ma and X. Yan, *ACS Nano*, 2018, **12**(8), 8266–8276.

43 T. Lin, X. Zhao, S. Zhao, H. Yu, W. Cao, W. Chen, H. Wei and H. Guo, *Theranostics*, 2018, **8**(4), 990–1004.
44 W. Zhen, Y. Liu, X. Jia, L. Wu, C. Wang and X. Jiang, *Nanoscale Horiz.*, 2019, **4**(3), 720–726.
45 Y. Liu, W. Zhen, L. Jin, S. Zhang, G. Sun, T. Zhang, X. Xu, S. Song, Y. Wang, J. Liu and H. Zhang, *ACS Nano*, 2018, **12**(5), 4886–4893.
46 Z. Zhou, J. Song, L. Nie and X. Chen, *Chem. Soc. Rev.*, 2016, **45**(23), 6597–6626.
47 Z. Ma, X. Jia, J. Bai, Y. Ruan, C. Wang, J. Li, M. Zhang and X. Jiang, *Adv. Funct. Mater.*, 2017, **27**(4), 1604258.
48 W. Zhen, Y. Liu, L. Lin, J. Bai, X. Jia, H. Tian and X. Jiang, *Angew. Chem., Int. Ed.*, 2018, **57**(32), 10309–10313.
49 J. Bai, X. Jia, W. Zhen, W. Cheng and X. Jiang, *J. Am. Chem. Soc.*, 2018, **140**(1), 106–109.
50 K. Liu, X. Liu, Q. Zeng, Y. Zhang, L. Tu, T. Liu, X. Kong, Y. Wang, F. Cao, S. A. G. Lambrechts, M. C. G. Aalders and H. Zhang, *ACS Nano*, 2012, **6**(5), 4054–4062.
51 T. Gallavardin, M. Maurin, S. Marotte, T. Simon, A. M. Gabudean, Y. Bretonniere, M. Lindgren, F. Lerouge, P. L. Baldeck, O. Stephan, Y. Leverrier, J. Marvel, S. Parola, O. Maury and C. Andraud, *Photochem. Photobiol. Sci.*, 2011, **10**(7), 1216–1225.
52 A. Kamkaew, F. Chen, Y. Zhan, R. L. Majewski and W. Cai, *ACS Nano*, 2016, **10**(4), 3918–3935.
53 T. Machleidt, C. C. Woodroofe, M. K. Schwinn, J. Méndez, M. B. Robers, K. Zimmerman, P. Otto, D. L. Daniels, T. A. Kirkland and K. V. Wood, *ACS Chem. Biol.*, 2015, **10**(8), 1797–1804.
54 K. Tanha, A. M. Pashazadeh and B. W. Pogue, *Biomed. Opt. Express*, 2015, **6**(68), 3053–3065.
55 Z. Wang, Y. Zhang, E. Ju, Z. Liu, F. Cao, Z. Chen, J. Ren and X. Qu, *Nat. Commun.*, 2018, **9**(1), 3334.
56 J. E. Kennedy, *Nat. Rev. Cancer*, 2005, **5**(4), 321–327.
57 S. Mitragotri, *Nat. Rev. Drug Discovery*, 2005, **4**(3), 255–260.
58 C. Dai, S. Zhang, Z. Liu, R. Wu and Y. Chen, *ACS Nano*, 2017, **11**(9), 9467–9480.
59 X. Pan, L. Bai, H. Wang, Q. Wu, H. Wang, S. Liu, B. Xu, X. Shi and H. Liu, *Adv. Mater.*, 2018, **30**(23), 1800180.
60 Z. Zhou, J. Song, L. Nie and X. Chen, *Chem. Soc. Rev.*, 2016, **45**(23), 6597–6626.
61 Y. Huang, J. Ren and X. Qu, *Chem. Rev.*, 2019, **119**(6), 4357–4412.
62 N. Yumita, Y. Iwase, K. Nishi, H. Komatsu, K. Takeda, K. Onodera, T. Fukai, T. Ikeda, S.-i. Umemura, K. Okudaira and Y. Momose, *Theranostics*, 2012, **2**(9), 880–888.
63 C. McEwan, C. Fowley, N. Nomikou, B. McCaughan, A. P. McHale and J. F. Callan, *Langmuir*, 2014, **30**(49), 14926–14930.
64 P. Zhu, Y. Chen and J. Shi, *ACS Nano*, 2018, **12**(4), 3780–3795.
65 L. J. Rich and M. Seshadri, *Radiology*, 2014, **275**(1), 110–118.
66 B. Ma, S. Wang, F. Liu, S. Zhang, J. Duan, Z. Li, Y. Kong, Y. Sang, H. Liu, W. Bu and L. Li, *J. Am. Chem. Soc.*, 2019, **141**(2), 849–857.
67 Z. Tang, Y. Liu, M. He and W. Bu, *Angew. Chem., Int. Ed.*, 2019, **58**(4), 946–956.
68 L. S. Lin, J. Song, L. Song, K. Ke, Y. Liu, Z. Zhou, Z. Shen, J. Li, Z. Yang, W. Tang, G. Niu, H. H. Yang and X. Chen, *Angew. Chem., Int. Ed.*, 2018, **57**(18), 4902–4906.
69 W. Ke, J. Li, F. Mohammed, Y. Wang, K. Tou, X. Liu, P. Wen, H. Kinoh, Y. Anraku, H. Chen, K. Kataoka and Z. Ge, *ACS Nano*, 2019, **13**(2), 2357–2369.
70 F. Liu, L. Lin, Y. Zhang, Y. Wang, S. Sheng, C. Xu, H. Tian and X. Chen, *Adv. Mater.*, 2019, 1902885.
71 A. L. Jackson, R. Chen and L. A. Loeb, *Proc. Natl. Acad. Sci. U. S. A.*, 1998, **95**(21), 12468.
72 M. Huo, L. Wang, Y. Chen and J. Shi, *Nat. Commun.*, 2017, **8**(1), 357.
73 S. E. Kim, L. Zhang, K. Ma, M. Riegman, F. Chen, I. Ingold, M. Conrad, M. Z. Turker, M. Gao, X. Jiang, S. Monette, M. Pauliah, M. Gonen, P. Zanzonico, T. Quinn, U. Wiesner, M. S. Bradbury and M. Overholtzer, *Nat. Nanotechnol.*, 2016, **11**(11), 977–985.
74 P. A. Ma, H. Xiao, C. Yu, J. Liu, Z. Cheng, H. Song, X. Zhang, C. Li, J. Wang, Z. Gu and J. Lin, *Nano Lett.*, 2017, **17**(2), 928–937.
75 C. Xu, Z. Yuan, N. Kohler, J. Kim, M. A. Chung and S. Sun, *J. Am. Chem. Soc.*, 2009, **131**(42), 15346–15351.
76 S. J. Dixon and B. R. Stockwell, *Nat. Chem. Biol.*, 2014, **10**(1), 9–17.
77 M. F. Poyton, A. M. Sendecki, X. Cong and P. S. Cremer, *J. Am. Chem. Soc.*, 2016, **138**(5), 1584–1590.
78 B. Ding, S. Shao, F. Jiang, P. Dang, C. Sun, S. Huang, P. Ma, D. Jin, A. A. A. Kheraif and J. Lin, *Chem. Mater.*, 2019, **31**(7), 2651–2660.
79 L. Wang, M. Huo, Y. Chen and J. Shi, *Biomaterials*, 2018, **163**, 1–13.
80 H. Ranji-Burachaloo, F. Karimi, K. Xie, Q. Fu, P. A. Gurr, D. E. Dunstan and G. G. Qiao, *ACS Appl. Mater. Interfaces*, 2017, **9**(39), 33599–33608.
81 L. Feng, R. Xie, C. Wang, S. Gai, F. He, D. Yang, P. Yang and J. Lin, *ACS Nano*, 2018, **12**(11), 11000–11012.
82 Z. Zhou, J. Song, R. Tian, Z. Yang, G. Yu, L. Lin, G. Zhang, W. Fan, F. Zhang, G. Niu, L. Nie and X. Chen, *Angew. Chem., Int. Ed.*, 2017, **129**(23), 6492–6496.
83 C. Wang, F. Cao, Y. Ruan, X. Jia, W. Zhen and X. Jiang, *Angew. Chem., Int. Ed.*, 2019, **58**(29), 9846–9850.